

VDMA
Fluid Power Association

22nd

ISC

International Sealing Conference

Stuttgart, Germany
October 01 - 02, 2024

Sealing Technology –
Challenges accepted!



© 2024 VDMA Fluidtechnik

All rights reserved. No part of this publication may be reproduced, stored in retrieval systems or transmitted in any form by any means without the prior permission of the publisher.

ISBN 978-3-8163-0768-6

Fachverband Fluidtechnik im VDMA e. V. Lyoner Str. 18
50628 Frankfurt am Main
Germany

Phone +49 69 6603-1513

E-Mail maximilian.baxmann@vdma.org

Internet www.vdma.org/fluid



Advancing Lubrication Calculation: A Physics-Informed Neural Network Framework for Transient Effects and Cavitation Phenomena in Reciprocating Seals

Faras Brumand-Poor, Florian Barlog, Nils Plückerhahn, Matteo Thebelt, Katharina Schmitz

In numerous technical applications, gaining insights into the behavior of tribological systems is crucial for optimizing efficiency and prolonging operational lifespans. Experimentally investigating these systems, such as reciprocating seals in fluid power systems, is expensive and time-consuming. An alternative is using elastohydrodynamic lubrication (EHL) simulation models, which however require extensive computational time. Physics-informed machine learning (PIML), particularly physics-informed neural networks (PINNs), offers an accelerated solution by integrating data-driven and physics-based methods into the training process to solve EHL's governing equations. This study demonstrates PINNs' capability to efficiently model tribological systems and accurately predict pressure dynamics and cavitation, showcasing their potential to enhance computational efficiency.

1 Introduction

The performance, efficiency, and durability of components in technical systems are significantly affected by their lubricated tribological contacts, such as those found in seals. Due to the complexity of the occurring phenomena in lubricated contacts, grasping a deeper understanding has proven to be a challenge. Especially, the dynamic friction, mainly described by fluid dynamics, is crucial for the accurate modeling of these contacts. Analytical model approaches are often not feasible without further simplification and neglect of certain phenomena, resulting in inaccurate models. Experimental measurements to obtain an understanding of the tribological behavior, are typically time-consuming and expensive. A commonly applied approach is modeling the system with an elastohydrodynamic lubrication (EHL) simulation, which employs the Reynolds equation to compute pressure distribution and the deformation of the contact surfaces.

An EHL simulation model for reciprocating seals, the ifas-DDS, was developed at the Institute for Fluid Power Drives and Systems of the RWTH Aachen (ifas). This model computes the friction by solving the hydrodynamics within the sealing contact, described by the Reynolds equation, and considering the contact mechanics and the seal deformation. In prior studies, the EHL model was validated with experimental

data [1]. A major limitation of this approach is the extensive computation time necessary to solve the underlying equations with numerical methods. Increasing computational resources might improve this issue, but is not always viable, particularly as simulation complexity grows and real-time computation for applications like control systems or digital twins is required.

Machine learning algorithms, like neural networks, represent a promising alternative to classical EHL simulations due to their fast computation ability after an initial training session. However, traditional neural networks are typically not implemented in such a manner that the underlying physical principles are integrated into the network. The main goal of the utilization of a neural network, typically in regression tasks, is to minimize the deviation of the network's prediction to a desired value. This purely data-based approach might result in a good prediction for the provided data but may lead to overfitting, which means that new data points inside the training domain and especially outside of it are predicted with a high error. An advancement in the field of neural networks is physics-informed neural networks (PINNs) tackling this challenge by incorporating physical laws into the network's training, thereby enhancing the networks' predictive accuracy and generalizability across unfamiliar data regimes. PINNs are a class of machine learning solvers for partial differential equations (PDEs). Their main distinguishment from the traditional neural network is, that their training process is not purely data-driven. The optimal parameter configuration of a given network structure is determined by the so-called loss, which is computed by data in the case of a conventional neural network. In the case of PINNs, the loss also incorporates physical laws underlying the investigated problem. The physical laws are described by initial and boundary conditions and the residuals of the PDEs. Several research has been conducted on the hydrodynamic part of EHL simulations, neglecting deformation and friction. Recent developments in this area like the studies by Almqvist [2] and others, showcase the potential of PINNs to combine the preciseness of distributed simulation models with the computational efficiency of neural networks, ensuring robust, accurate, and faster computations.

This contribution demonstrates the capability of PINNs to solve the Reynolds equation with dynamic contact geometry changes and cavitation modeling applied to sealing contact with housing. For this investigation, a hydrodynamic-PINN (HD-PINN) framework, which has previously been validated for stationary scenarios without cavitation [3], is applied. This framework is extended and applied to two scenarios. Firstly, a dynamic change of the investigated gap height and secondly a divergent gap with cavitation. Like the prior mentioned studies, this work focuses on the hydrodynamic part of the EHL. It focuses on computing the pressure and cavitation distribution while neglecting friction and contact mechanics. Deformation is artificially

modeled by a constant movement of the seal, neglecting any pressure dependencies. The following section presents the considered model for hydrodynamic lubrication. In section 3, PINNs are described in general. The subsequent section 4 presents the HD-PINN framework, the extensions applied to it, the two investigated scenarios, and the physics-based losses. Subsequently, the results of the PINNs are shown and validated by a modified version of the ifas-DDS, referred to as the rigid DDS, neglecting the prior mentioned factors of the EHL. Eventually, a summary and conclusion are provided in section 6.

2 Hydrodynamic Lubrication

Modeling tribological systems by EHL simulations is a common approach to obtaining a detailed description of friction, leakage, and wear within lubricated mechanical interfaces. EHL models assess the dynamic relationship between surfaces in contact with lubricants, resolving the surface deformation and the hydrodynamic pressure within the contact area. These simulations are essential tools for designing and optimizing tribological contacts in various technical applications.

The ifas-DDS is a distributed parameter simulation model, which simulates complex interactions between a reciprocating seal and its mating countersurface. One essential aspect of this simulation is the consideration of a lubricant, which separates the sealing and the housing and allows a characterization of the sealing behavior. The model consists of two main parts, first the deformation determined by the finite element software Abaqus and second the hydrodynamic part described by the Reynolds equation, which is integrated into Abaqus via user subroutines.

The focus of this research lies in solving the Reynolds equation, therefore simplifying the model by neglecting the deformation of the contacting surfaces, the contact mechanics, and the friction. Within the scope of this research, the investigation focuses on hydrodynamic lubrication. Therefore, the rigid DDS is employed instead of the ifas-DDS.

In this study, the PINN is validated by the rigid DDS. This comparison focuses on the solution process of two solvers for the same set of equations, namely the Reynolds equation and the Fischer-Burmeister equation. The DDS extends the Reynolds equation by the flow factors ϕ^r and ϕ^p as described by Patir and Cheng [4], thus allowing the consideration of surface topography effects on the hydrodynamic lubrication. Furthermore, the cavitation is modeled by integrating the Jakobsson-Floberg-Olsson equation, which introduces the cavitation fraction θ to consider the formation of the gaseous phase, e.g., due to vaporization of solved air in the lubricant due to localized pressure drops [5]. The cavitation fraction describes the gaseous phase's local volume fraction between 0 at no cavitation to 1 for full cavitation.

The original Reynolds equation, as stated by Osborne Reynolds in 1886 is extended to model the cavitation. It is implemented into the DDS and is detailed as follows [6]:

$$\frac{v}{2} \frac{\partial}{\partial x} \left((1 - \theta) \rho h R_q \Phi^\tau \right) - \frac{1}{12\eta} \frac{\partial}{\partial x} \left(\Phi^v \rho h^3 \frac{\partial p}{\partial x} \right) + \frac{\partial}{\partial t} \left((1 - \theta) \rho h \right) = 0 \quad (1)$$

Cavitation occurs when the pressure drops below the vaporization pressure which is assumably zero in this work [7]. To describe the relation between pressure and cavitation, the Fischer-Burmeister equation is used:

$$p + \theta - \sqrt{p^2 + \theta^2} = 0 \quad (2)$$

The Jakobsson-Floberg-Olsson cavitation model can be used to track the lubrication distribution in tribological contacts with a limited amount of lubrication supply (starved lubrication), namely grease lubricated sealing contacts in pneumatic spool valves. Due to this modeling, a cavity fraction unequal zero does not necessarily describe the occurrence of cavitation but a partial filled sealing gap at the corresponding position. A better interpretation is obtained by introducing the lubricant film height h_{lub} , which is calculated from h and θ :

$$h_{lub} = (1 - \theta) h \quad (3)$$

3 Physics-Informed Neural Networks

The previously introduced Reynolds equation describes the pressure distribution in lubricated contacts. When an analytical solution is not available, methods such as finite volume, elements, or differences are often used to solve tribological problems. As these methods are often computationally intensive and time-consuming, machine learning methods have shown promise in the past and are becoming increasingly important in the field of tribology [8, 9].

Machine learning models, often referred to as black-box models, are typically data-driven and advantageous due to their simplicity and adaptability. However, since their inception, hybrid models, which combine ideas from physics with data-driven methodologies, have become increasingly important. These models benefit from the common lack of adequate measurement data and a thorough mathematical description of the system, which makes data-driven and solely physics-based (white-box)

modeling approaches unfeasible [10]. Over time, several different hybrid model configurations have been investigated, including sequential, parallel, and structured forms [11–13].

The development of hybrid models represents a promising advancement in the field of tribology, which is physics-informed machine learning (PIML). PIML is employed in tribology for a multitude of purposes, including the estimation of wear or damage and the evaluation of lubrication conditions in hydrodynamic interfaces. In contrast to traditional machine learning techniques, which predominantly utilize data-driven approaches (black-box models), PIML, particularly when utilizing PINNs, integrates physical principles to direct the learning procedure. Consequently, the outputs generated by these models are frequently both more accurate and dependable than those obtained by data-driven methods [14]. A PINN can be conceptualized as a hybrid model in contrast to the previously discussed models. It employs a neural network as the prediction model and incorporates residual terms into the loss function during training to integrate information from physical laws [15].

Hyuk [16] and Lagaris [17] did the fundamental work in physics-based regularization of neural networks after Cybenko [18] and Hornik [19] provided the necessary evidence that neural networks can be used as universal function approximators. Although Hyuk and Lagaris did not specifically use the term "physics-informed" in their study, their goals are similar to the ideas that are now recognized as the foundation of PINNs. Hyuk's method laid the foundation for the later field of PINNs by extending the loss function of the neural network to include the governing differential equation. Because computer resources were limited and computational algebra techniques were still in their infancy, the idea of combining physical rules with neural network training initially received little attention. However, with the advancement in hardware capabilities and the emergence of effective gradient computation methodologies, such as automatic differentiation, this theory has experienced a resurgence.

In 2014, Owhadi was the first to reintroduce PIML, integrating past knowledge into the problem-solving process. He proposed that algorithms be enhanced by incorporating prior information and formulating PDE solutions as Bayesian inference problems [20]. Building upon these premises, Raissi and colleagues employed a probabilistic machine learning technique to solve general linear equations using Gaussian processes, tailoring it particularly for integro-differential or partial differential equations [21, 22]. To address the challenge of solving nonlinear partial differential equations, this technique was subsequently expanded [23, 24]. Moreover, a noteworthy development was the creation of the PINN, which are mesh-free models that restructure the solution of PDEs into a loss function optimization problem [25]. To handle forward and inverse problems given by PDEs, Raissi presented PINNs, a new class of hybrid solvers [26–28]. In Figure 1 an exemplary PINN is shown.

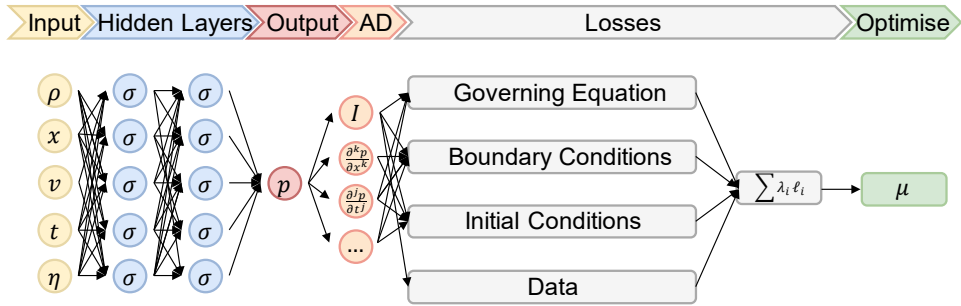


Figure 1: An exemplary PINN.

PINNs process their inputs (such as case-dependent parameters or position x and time t) the same way as traditional neural networks. The values are processed by a multitude of layers to get the network's output. In each layer, multiple neurons are connected to the ones of the previous and next layer. Each neuron executes mathematical operations like multiplying its inputs by a weight, adding a bias, and passing the result to an activation function to calculate its individual output. The sum of all these operations leads to the neural network's ability to predict complex functions as its total output.

The residual losses correspond to the residuals of the governing (physic) equations and thus is an unsupervised loss [14]. This loss is evaluated for specific spatial and, depending on the problem, time points, which are the so-called collocation points in position n_x and time n_t . To integrate complex differential equations, the implementation of automatic differentiation in neural networks is exploited. This method efficiently computes gradients of any order [29] with machine accuracy by applying differential rules such as chain and product rules. In traditional neural networks, automatic differentiation is used to calculate gradients for the update of the parameters, while in PINNs it can additionally be used to calculate derivatives for differential equations.

The boundary condition (BC) and initial condition (IC) losses are used to ensure that the boundary and initial conditions are compliant with given targets. Hence, these two losses are supervised losses. It can be seen in Figure 1 that additional losses can occur. The example in that figure is a so-called hybrid PINN, which uses existing data for the given equations to contribute to a faster or more accurate solution. Therefore, a data loss, which corresponds to the classical data-driven loss, is added.

Before introducing the methods and loss function used in this work in detail, the next section gives a brief overview of the use of PINNs in hydrodynamics.

The first publication to use PINNs for solving a simplified Reynolds equation was released by Almqvist in 2021 [2]. Over the next years, these ideas were expanded by Zhao et al., Li et al., and Yadav et al. who further developed a method to solve the 2D Reynolds equation for more complex problems [30–32]. Notable further progress was made by Rom who first used PINNs for solving the stationary Reynolds equation with the Jakobsson-Floberg-Olsson (JFO) cavitation model. He also introduced soft constraints and collocation point updates to improve cavitation distributions in general but especially in areas with high gradients [33].

Additional advancements were made by Cheng et al., who used PINNs to solve the Reynolds equation for the JFO and Swift-Stieber (SS) cavitation models [34]. Xi et al. further enhanced the solution of PINNs by using hard and soft constraints [35].

Brumand et al. established that one PINN is sufficient to learn the solution of the stationary Reynolds equation for a multitude of different parameters, such as boundary conditions [36].

A step towards using PINNs for a complete EHL simulation was done by Rimon et al. who used a simplified Reynolds equation as well as the Lamé equation for the description of the seal deformation [37].

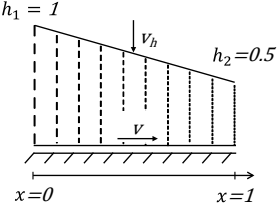
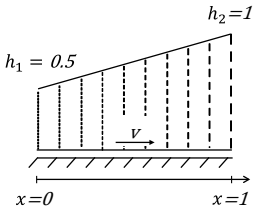
Although the previously mentioned contributions show immanent progress in solving the complete Reynolds equation, it must be noted that most of these publications were focused on the implementation of PINNs themselves rather than on developing a hydrodynamic lubrication PINN framework. Thus, a significant amount of research and work must be done to solve the complete Reynolds equation in a way that can be used for the replacement of an EHL simulation.

4 HD-PINN Framework

4.1 Test Cases: Physics-Informed Loss and Conditions

In this work, two special cases are investigated. Both scenarios are listed in Table 1. Firstly, the sealing movement and secondly the stationary cavitation are presented, afterwards the training procedure and the framework are briefly described.

Table 1: Investigated test scenarios.

Scenario	$\theta \neq 0$	$\frac{\partial \cdot}{\partial t}$	v	BCs	Gap Geometry
Sealing Movement	\times	$\frac{\partial \theta}{\partial t} = 0$ $\frac{\partial h}{\partial t} = -0.1$	0.1	$p_{left} = 0.3$ $p_{right} = 0.2$ $\theta_{left} = 0$ $\theta_{right} = 0$	
Stationary Cavitation	\checkmark	$\frac{\partial \theta}{\partial t} = 0$ $\frac{\partial h}{\partial t} = 0$	1	$p_{left} = 0.7$ $p_{right} = 0.2$ $\theta_{left} = 0$ $\theta_{right} = 0$	

4.1.1 Sealing Movement

For the first test case, a converging gap is analyzed. The housing, as the bottom part, moves horizontally in a shearing motion relative to the top part which represents the seal. In addition, the seal is moved vertically towards the housing with the idea in mind to model a simple way of deformation without any interaction with the actual pressure distribution. In this converging setup, no cavitation is modeled.

The Reynolds equation for this specific case is shown in Equation (4). For both scenarios, smooth surfaces and incompressible fluids are assumed, which leads to the neglect of the roughness R_q , the flow factors ϕ^τ and ϕ^r and the density ρ .

$$\frac{v}{2} \frac{\partial h}{\partial x} - \frac{1}{12\eta} \frac{\partial}{\partial x} \left(h^3 \frac{\partial p}{\partial x} \right) + \frac{\partial h}{\partial t} = 0 \quad (4)$$

To solve the Reynolds equation for this specific case, pressure boundary conditions are required. Since the lubricant is incompressible and the seal is moved with a constant velocity, no transient effects are present. Hence the PINN's losses consist of the residual and boundary condition loss being implemented as Mean Squared Error (MSE) terms, which is a common choice for PINNs. Simulation parameters are shown in and the PINN with an exemplary network structure is depicted in Figure 2.

Table 2: Simulation parameters for the sealing movement scenario.

Variable	Value	Variable	Value
n_x	100	v_{rel}	0.1
n_t	10	v_h	-0.1
p_{left}, p_{right}	0.3, 0.2	h	[1, 0.5, 0, 0]

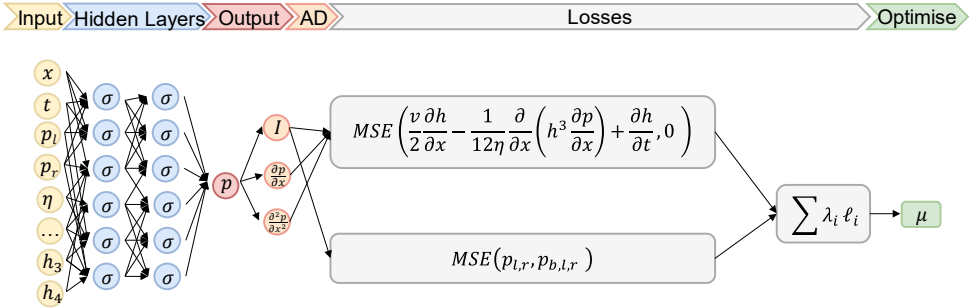


Figure 2: PINN for the sealing movement scenario.

4.1.2 Stationary Cavitation

In the second test case, cavitation is modelled and therefore a diverging gap is chosen. Similar to the first case, the housing is moved horizontally but the seal is fixed. Since cavitation is modelled, the losses consist of the already introduced residual loss and boundary conditions loss but need further extension by the Fischer-Burmeister loss. Rom demonstrated that the Fischer-Burmeister loss itself is insufficient to model transitions between cavitated and non-cavitated areas adequately and therefore introduced soft constraints [33]. These are implemented as a fourth condition to train the PINN. The set simulation parameters and the PINN are shown in Table 3 and Figure 3, respectively.

Table 3: Simulation parameters for the stationary cavitation scenario

Variable	Value	Variable	Value
n_x	400	h	[0.5, 1, 0, 0]
n_t	1	p_{thresh}	0.005
p_{left}, p_{right}	0.7, 0.2	θ_{thresh}	0.1
$\theta_{left}, \theta_{right}$	0, 0	$\left(\frac{\partial \theta}{\partial x}\right)_{thresh}$	15
v_{rel}	1	n_{CP_added}	15
v_h	0		

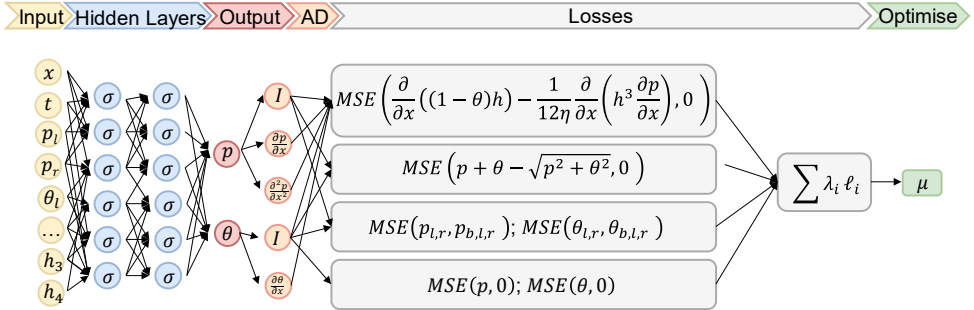


Figure 3: PINN Architecture in case of Cavitation.

Since a stationary model is built, transient effects are neglected. Therefore, the Reynolds equation is as follows:

$$\frac{\partial}{\partial x}((1 - \theta)h) - \frac{1}{12\eta} \frac{\partial}{\partial x} \left(h^3 \frac{\partial p}{\partial x} \right) = 0 \quad (5)$$

To enforce the Fischer-Burmeister equation being fulfilled in transition areas especially, the soft constraints loss is implemented in the following two equations:

$$\theta = 0, \quad \text{if } p > p_{thresh} \quad (6)$$

$$p = 0, \quad \text{if } \theta > \theta_{thresh} \quad (7)$$

Pressure and cavitation should never be non-zero at the same position. Therefore, thresholds are introduced: Whenever one threshold is exceeded, values of the corresponding pressure or cavitation are returned as a loss. Since these transition areas usually make up for a small portion of the whole domain, these areas are considered when normalizing the loss.

4.2 Training Procedure

The framework consists of three main parts, shown in Figure 4: The PINN itself and two optimizers. While the Bayesian optimizer improves the fundamental hyperparameters, initializing a new network each iteration of an outer loop, the Adam optimizer updates the weights and biases of all neurons and therefore improves losses in an inner training loop. In each training iteration, the PINN is evaluated for returning pressure (and cavitation) predictions, and the corresponding losses are calculated. When the final epoch is finished, the Bayesian optimization computes new hyperparameters for the next trial.

Once promising hyperparameters are found, training without Bayesian optimization and a higher number of epochs is started. The final model is saved for evaluation.

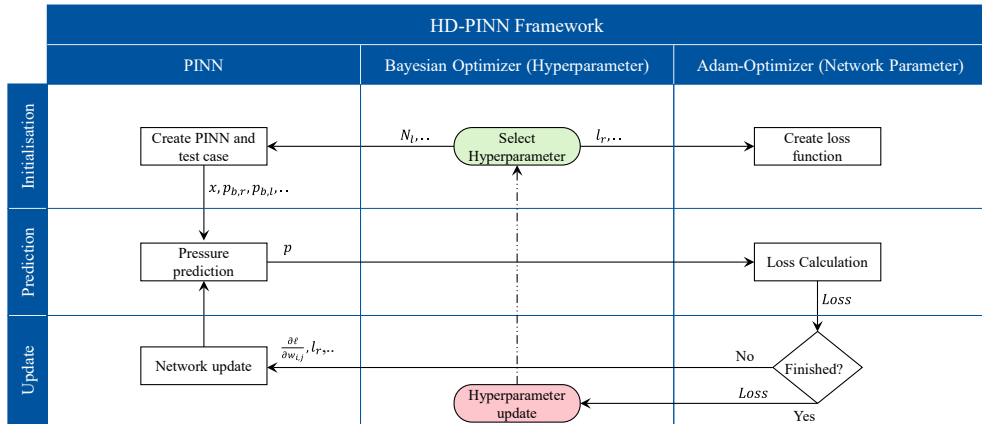


Figure 4: HD-PINN framework for the training procedure. Adapted from [36].

4.3 Adaptive Collocation Points

Areas with high θ -gradients have shown to be hard to predict and therefore need special refinement [33]: After training the neural network for 50000 epochs, new collocation points n_x are added in desired areas. Gradients are checked whether they exceed a certain threshold, and if so a predefined number of 15 collocation points is added to their left. This process is repeated every 5000 epochs until a total of four updates is reached. This ensures that a region with high gradients is sufficiently sampled to obtain an adequate resolution of these areas.

5 Results

5.1 Sealing Movement

The pressure distribution of PINN and DDS for three different time steps, $t = (0, 0.5, 1)$ of the first scenario and the initial seal geometry are shown in Figure 5. The PINN shows good agreement with the DDS for the pressure trajectory for each time step. The pressure increase over time is accurately captured by the PINN.

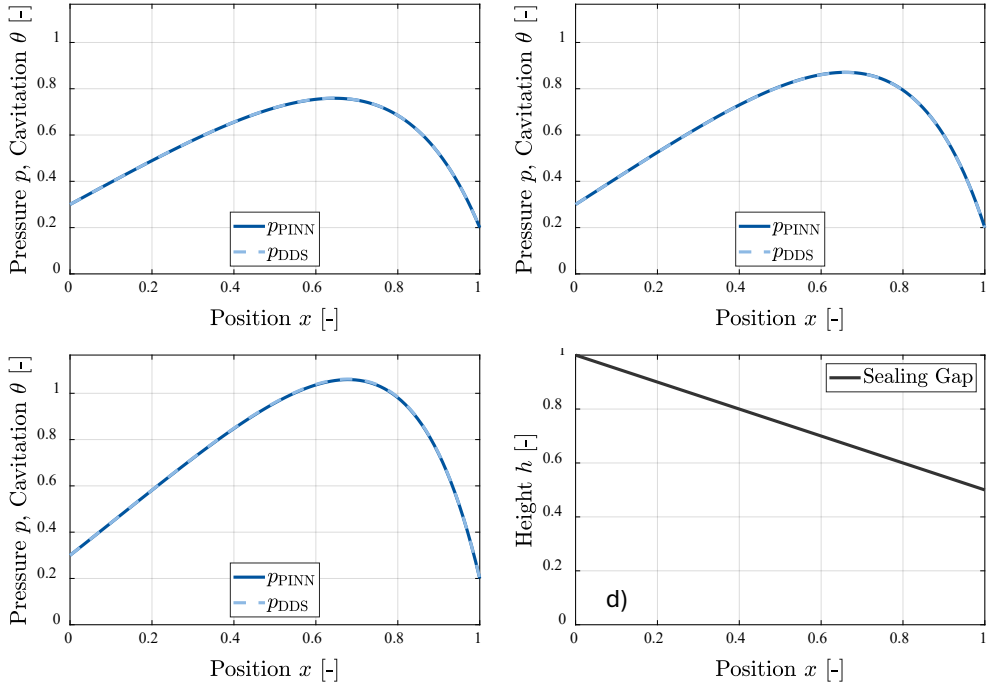


Figure 5: Pressure distribution for the sealing movement scenario for a) $t = 0$, b) $t = 0.5$, c) $t = 1$ and d) the sealing geometry at $t = 0$.

5.2 Stationary Cavitation

The results of the second scenario, the stationary cavitation, are depicted in Figure 6. The results show the pressure distribution and the cavitation fraction in one plot and the lubrication film height in another plot.

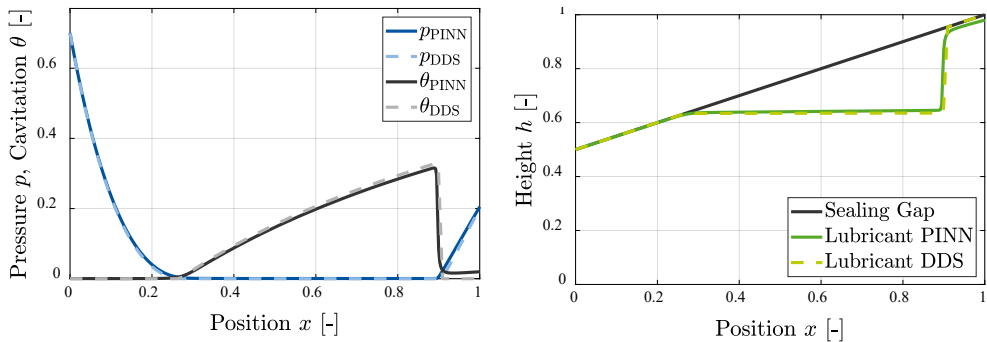


Figure 6: Pressure distribution and cavitation for the stationary cavitation scenario and the lubrication height.

In the second scenario, the PINN also performs well for the pressure distribution and the cavitation area. The right transition regime shows some deviation between PINN and DDS. The soft constraints enhance the location of the switch between pressure and cavitation area. Further tuning of the constraints in combination with new hyperparameters could increase the accuracy even more.

6 Summary and Conclusion

This contribution demonstrates the capability of PINNs to solve dynamic height changes and cavitation modeling tasks, governed by the Reynolds equation. They do so, by computing the pressure distribution and cavitation fraction within sealing contacts in a housing. In the beginning, an introduction to hydrodynamic lubrication was given, followed by a description of PINNs and their application-solving variants of the Reynolds equation. After that, the investigated scenarios of sealing movement and stationary cavitation as well as the applied training procedure for the PINNs were presented in detail.

Regarding the pressure, the PINN can accurately compute the distribution and the boundaries, validated with the DDS. The cavitation determination in the second scenario demonstrates good agreement inside the cavitation region. For the regime where pressure and cavitation area switch, the PINN can locate them and sufficiently compute the desired values. The PINN showed the possibility of computing high gradients, and the introduced soft constraints represent a further possibility for increasing accuracy in these areas. The results of this work represent an advancement in the domain of lubricated contact simulations, depicting a PIML approach to accelerate hydrodynamic lubrication computation with no to less accuracy loss.

Further work will be done by integrating transient behavior for the cavitation fraction of the Reynolds equation and solving this scenario with the framework. Additionally, the soft constraints will be investigated to obtain more accuracy for high-gradient regions.

7 Acknowledgements

The authors thank the Research Association for Fluid Power of the German Engineering Federation VDMA for its financial support. Special gratitude is expressed to the participating companies and their representatives in the accompanying industrial committee for their advisory and technical support.

8 Nomenclature

Variable	Description	Unit
h	Gap height	[-]
h_{lub}	Lubrication height	[-]
h_1	Height at left end	[-]
h_2	Height at right end	[-]
h_3	Curvature of sealing	[-]
h_4	Position for sealing bend	[-]
n_t	Time collocation points	[-]
n_x	Position collocation points	[-]
p	Hydrodynamic pressure	[-]
$p_{b,l,r}$	Pressure boundary condition for left and right boundary	[-]
$p_{l,r}$	Pressure at the left and right boundary	[-]
p_{thersh}	Pressure threshold for soft constraints	[-]
R_q	Root mean squared contact surface roughness	[-]
t	Time	[-]
v	Velocity of counter surface	[-]
v_h	Velocity of sealing	[-]
x	Axial coordinate	[-]
x_b	Position of sealing bend	[-]
x_l	Left end of the geometry	[-]
x_r	Right end of the geometry	[-]
η	Fluid viscosity	[-]
θ	Cavity friction	[-]
θ_{thersh}	Cavitation threshold for soft constraints	[-]
ρ	Fluid density	[-]
ϕ^p	Pressure flow factors	[-]
ϕ^t	Shear flow factors	[-]
$\frac{\partial \cdot}{\partial x, t}$	Partial differentiation regarding time and position	[-]

9 REFERENCES

- [1] Bauer, N.; Sumbat, B.; Feldmeth, S.; Bauer, F.; Schmitz, K. Experimental determination and EHL simulation of transient friction of pneumatic seals in spool valves. *Sealing technology - old school and cutting edge : International Sealing Conference : 21st ISC*, **2022**, 503–522.
- [2] Almqvist, A. Fundamentals of Physics-Informed Neural Networks Applied to Solve the Reynolds Boundary Value Problem. *Lubricants*, **2021**, *9*, 82.
- [3] Brumand-Poor, F.; Bauer, N.; Plückhahn, N.; Schmitz, K. *Fast Computation of Lubricated Contacts: A Physics-Informed Deep Learning Approach*: Dresden, Germany, **March 19-21**.
- [4] Bauer, N.; Baumann, M.; Feldmeth, S.; Bauer, F.; Schmitz, K. Elastohydrodynamic Simulation of Pneumatic Sealing Friction Considering 3D Surface Topography. *Chem Eng & Technol*, **2023**, *46*, 167–174.
- [5] Bauer, N.; Rambaks, A.; Müller, C.; Murrenhoff, H.; Schmitz, K. Strategies for Implementing the Jakobsson-Floberg-Olsson Cavitation Model in EHL Simulations of Translational Seals. *TJFP*, **2021**.
- [6] Angerhausen, J.; Woyciniuk, M.; Murrenhoff, H.; Schmitz, K. Simulation and experimental validation of translational hydraulic seal wear. *Tribology International*, **2019**, *134*, 296–307.
- [7] Liu, X.; Wu, Z.; Li, B.; Zhao, J.; He, J.; Li, W.; Zhang, C.; Xie, F. Influence of inlet pressure on cavitation characteristics in regulating valve. *Engineering Applications of Computational Fluid Mechanics*, **2020**, *14*, 299–310.
- [8] Marian, M.; Tremmel, S. Current Trends and Applications of Machine Learning in Tribology—A Review. *Lubricants*, **2021**, *9*, 86.
- [9] Paturi, U.M.R.; Palakurthy, S.T.; Reddy, N.S. The Role of Machine Learning in Tribology: A Systematic Review. *Arch Computat Methods Eng*, **2023**, *30*, 1345–1397.
- [10] Velioglu, M.; Mitsos, A.; Dahmen, M. Physics-Informed Neural Networks (PINNs) for Modeling Dynamic Processes Based on Limited Physical Knowledge and Data. *2023 AIChE Annual Meeting*, **2023**.
- [11] Psychogios, D.C.; Ungar, L.H. A hybrid neural network-first principles approach to process modeling. *AIChE Journal*, **1992**, *38*, 1499–1511.
- [12] Su, H.-T.; Bhat, N.; Minderman, P.A.; McAvoy, T.J. Integrating Neural Networks with First Principles Models for Dynamic Modeling. *IFAC Proceedings Volumes*, **1992**, *25*, 327–332.
- [13] Kahrs, O.; Marquardt, W. The validity domain of hybrid models and its application in process optimization. *Chemical Engineering and Processing: Process Intensification*, **2007**, *46*, 1054–1066.

-
- [14] Cai, S.; Mao, Z.; Wang, Z.; Yin, M.; Karniadakis, G.E. Physics-informed neural networks (PINNs) for fluid mechanics: a review. *Acta Mech. Sin.*, **2021**, *37*, 1727–1738.
- [15] Nabian, M.A.; Meidani, H. Physics-Driven Regularization of Deep Neural Networks for Enhanced Engineering Design and Analysis. *Journal of Computing and Information Science in Engineering*, **2020**, *20*, 436.
- [16] Lee, H.; Kang, I.S. Neural algorithm for solving differential equations. *Journal of Computational Physics*, **1990**, *91*, 110–131.
- [17] Lagaris, I.E.; Likas, A.; Fotiadis, D.I. Artificial Neural Networks for Solving Ordinary and Partial Differential Equations. *IEEE Trans. Neural Netw.*, **1998**, *9*, 987–1000.
- [18] Cybenko, G. Approximation by superpositions of a sigmoidal function. *Math. Control Signal Systems*, **1989**, *2*, 303–314.
- [19] Hornik, K.; Stinchcombe, M.; White, H. Multilayer feedforward networks are universal approximators. *Neural Networks*, **1989**, *2*, 359–366.
- [20] Owhadi, H. *Bayesian Numerical Homogenization*, **June 25, 2014**.
- [21] Raissi, M.; Perdikaris, P.; Karniadakis, G.E. *Inferring solutions of differential equations using noisy multi-fidelity data*, **2016**.
- [22] Raissi, M.; Perdikaris, P.; Karniadakis, G.E. *Machine learning of linear differential equations using Gaussian processes*, **2017**.
- [23] Raissi, M.; Perdikaris, P.; Karniadakis, G.E. *Numerical Gaussian Processes for Time-dependent and Non-linear Partial Differential Equations*, **March 29, 2017**.
- [24] Raissi, M.; Karniadakis, G.E. Hidden physics models: Machine learning of nonlinear partial differential equations. *Journal of Computational Physics*, **2018**, *357*, 125–141.
- [25] Cuomo, S.; Di Cola, V.S.; Giampaolo, F.; Rozza, G.; Raissi, M.; Piccialli, F. Scientific Machine Learning Through Physics-Informed Neural Networks: Where we are and What's Next. *J Sci Comput*, **2022**, *92*.
- [26] Raissi, M.; Perdikaris, P.; Karniadakis, G.E. *Physics Informed Deep Learning (Part I): Data-driven Solutions of Nonlinear Partial Differential Equations*, **November 28, 2017**.
- [27] Raissi, M.; Perdikaris, P.; Karniadakis, G.E. *Physics Informed Deep Learning (Part II): Data-driven Discovery of Nonlinear Partial Differential Equations*, **November 28, 2017**.
- [28] Raissi, M.; Perdikaris, P.; Karniadakis, G.E. Physics-informed neural networks: A deep learning framework for solving forward and inverse problems involving nonlinear partial differential equations. *Journal of Computational Physics*, **2019**, *378*, 686–707.

-
- [29] Baydin, A.G.; Pearlmutter, B.A.; Radul, A.A.; Siskind, J.M. Automatic differentiation in machine learning: a survey. *Atilim Gunes Baydin*.
- [30] Zhao, Y.; Guo, L.; Wong, P.P.L. Application of physics-informed neural network in the analysis of hydrodynamic lubrication. *Friction*, **2023**, *11*, 1253–1264.
- [31] Li, L.; Li, Y.; Du, Q.; Liu, T.; Xie, Y. ReF-nets: Physics-informed neural network for Reynolds equation of gas bearing. *Computer Methods in Applied Mechanics and Engineering*, **2022**, *391*, 114524.
- [32] Yadav, S.K.; Thakre, G. Solution of Lubrication Problems with Deep Neural Network. In: *Advances in Manufacturing Engineering*. Dikshit, M.K., Soni, A., Davim, J.P., Eds.; Springer Nature Singapore: Singapore, **2023**; pp. 471–477.
- [33] Rom, M. Physics-informed neural networks for the Reynolds equation with cavitation modeling. *Tribology International*, **2023**, *179*, 108141.
- [34] Cheng, Y.; He, Q.; Huang, W.; Liu, Y.; Li, Y.; Li, D. HL-nets: Physics-informed neural networks for hydrodynamic lubrication with cavitation. *Tribology International*, **2023**, *188*, 108871.
- [35] Xi, Y.; Deng, J.; Li, Y. A new method to solve the Reynolds equation including mass-conserving cavitation by physics informed neural networks (PINNs) with both soft and hard constraints. *Friction*, **2024**.
- [36] Brumand-Poor, F.; Bauer, N.; Plückhahn, N.; Thebelt, M.; Woyda, S.; Schmitz, K. Extrapolation of Hydrodynamic Pressure in Lubricated Contacts: A Novel Multi-Case Physics-Informed Neural Network Framework. *Lubricants*, **2024**, *12*, 122.
- [37] Rimon, M.T.I.; Hassan, M.F.; Lyathakula, K.R.; Cesmeci, S.; Xu, H.; Tang, J. In: *ASME Power Applied R&D 2023*, ASME Power Applied R&D 2023, Long Beach, California, USA, 06.08.2023 - 08.08.2023; American Society of Mechanical Engineers, **2023**.

10 Authors

RWTH Aachen University, Institute for Fluid Power Drives and Systems (ifas)

Campus-Boulevard 30, 52074 Aachen, Germany:

Faras Brumand-Poor M. Sc., M. Sc., ORCID 0009-0006-7442-8706,
faras.brumand@ifas.rwth-aachen.de

Florian Barlog B. Sc., ORCID 0009-0006-4275-5825,
florian.barlog@ifas.rwth-aachen.de

Nils Plückerhahn B. Sc., ORCID 0009-0000-0789-6194,
nils.plueckhahn@ifas.rwth-aachen.de

Matteo Thebelt B. Sc., ORCID 0009-0005-8262-3053,
matteo.thebelt@ifas.rwth-aachen.de

Univ.-Prof. Dr.-Ing. Katharina Schmitz, ORCID 0000-0002-1454-8267,
katharina.schmitz@ifas.rwth-aachen.de

<https://doi.org/10.61319/J7I2HNKR>